Lecture 18
Applications of Auger spectroscopy

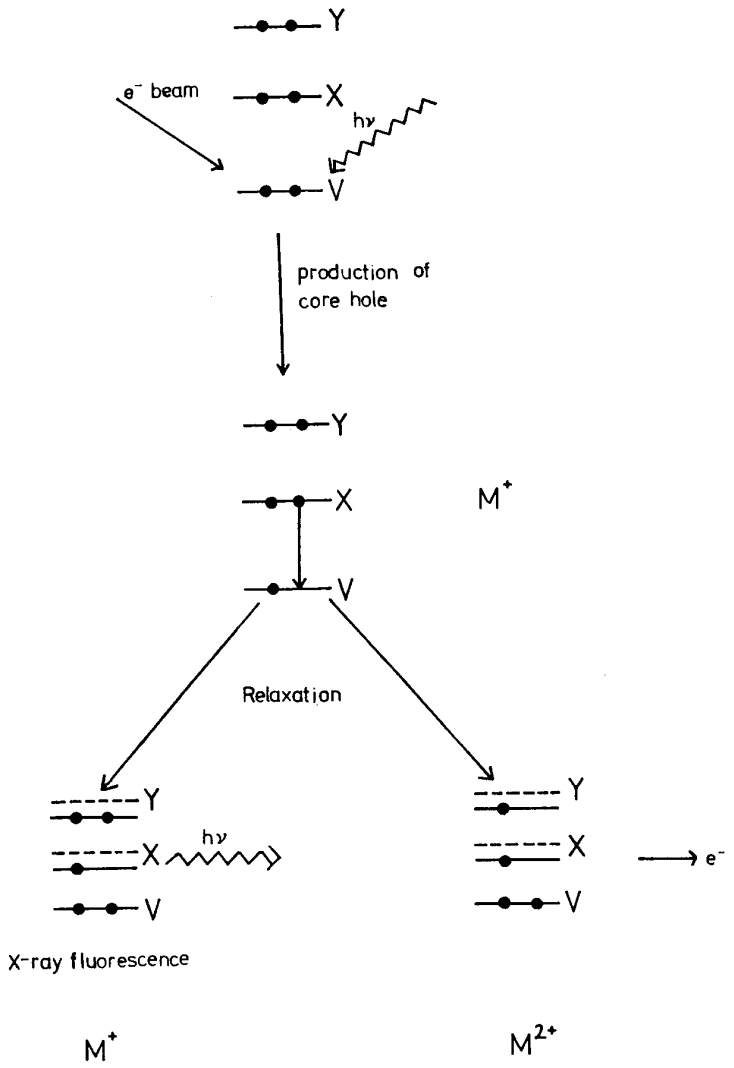

Figure 1.4. Possibilities for decay of a core vacancy.

Relaxation occurs as a result of core hole emission

The change of LS – jj coupling schemes

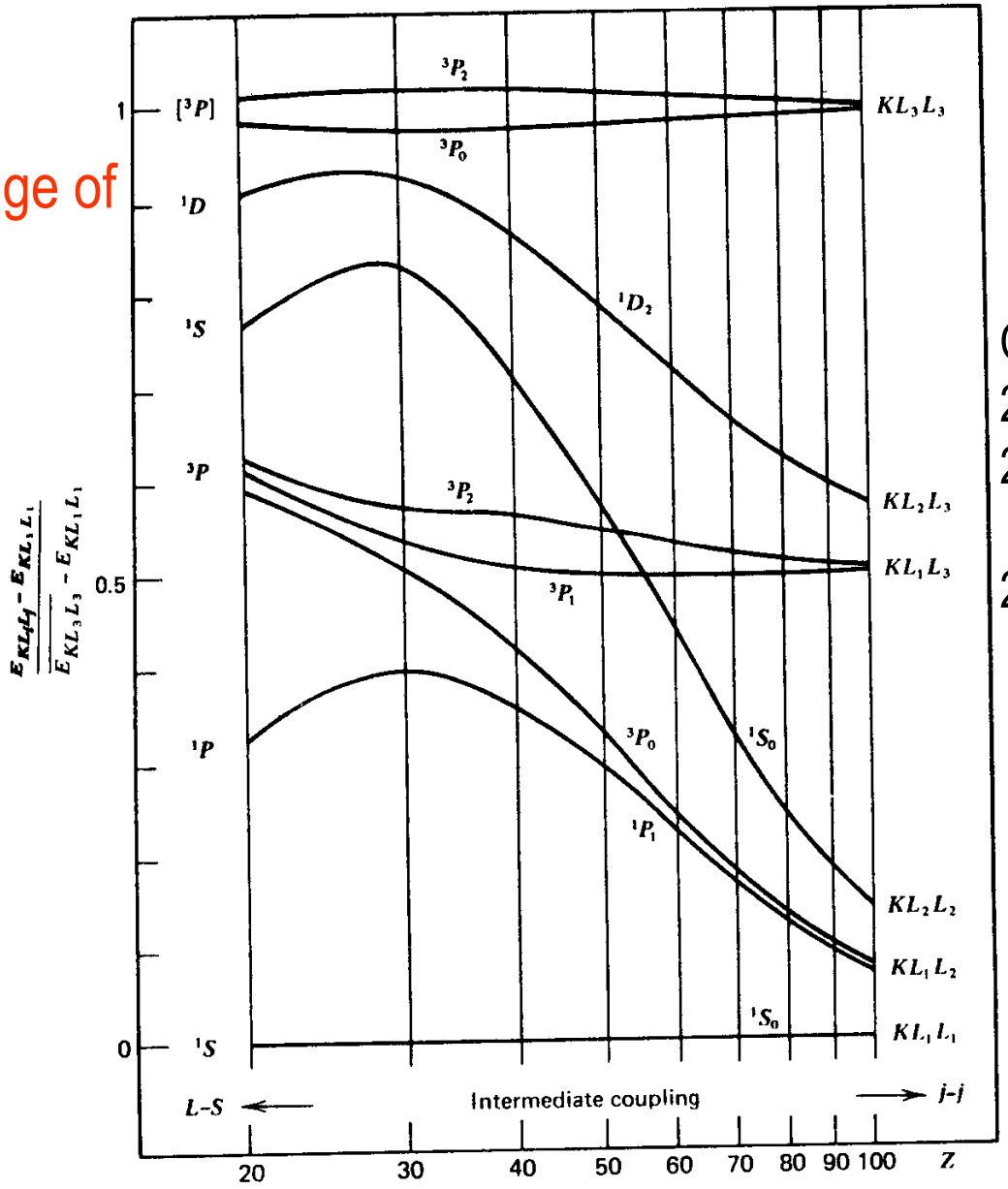

Figure 2.1. Coupling between final atomic vacancy states following a KLL transition for different Z. (Reprinted with permission of Wiley-Interscience, New York.)

Configurations

$2s^0 2p^6$	KL_1L_1	$1s2s2s$
$2s^1 2p^5$	KL_1L_2	$1s2s2p_{1/2}$
	KL_1L_3	$1s2s2p_{3/2}$
$2s^2 2p^4$	KL_2L_2	$1s2p_{1/2}2p_{1/2}$
	KL_2L_3	$1s2p_{1/2}2p_{3/2}$
	KL_3L_3	$1s2p_{3/2}2p_{3/2}$

Details of the electronic structure can be studied

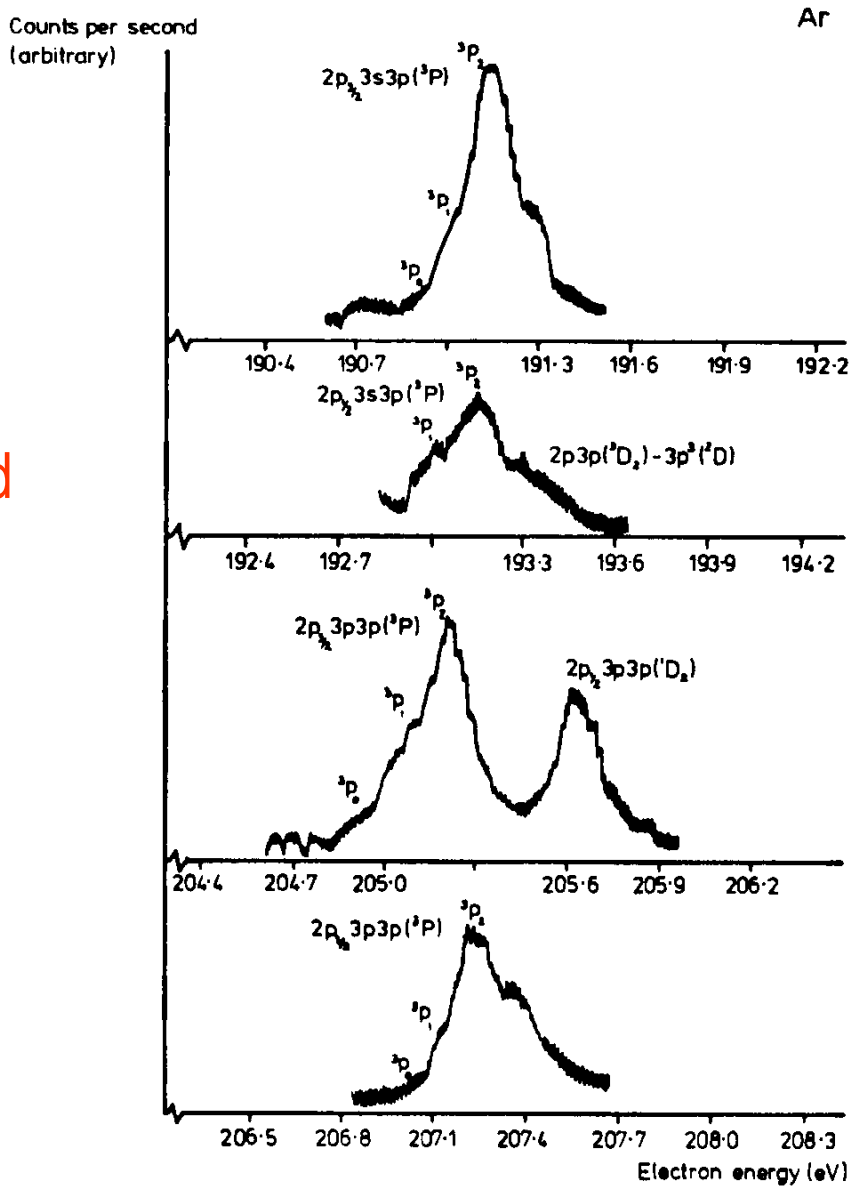

Figure 2.2. Auger ^3P peaks of argon in the gas phase by electron impact.[5] (Reprinted with permission of American Chemical Society, Washington.)

Variation in intensity with change in excitation

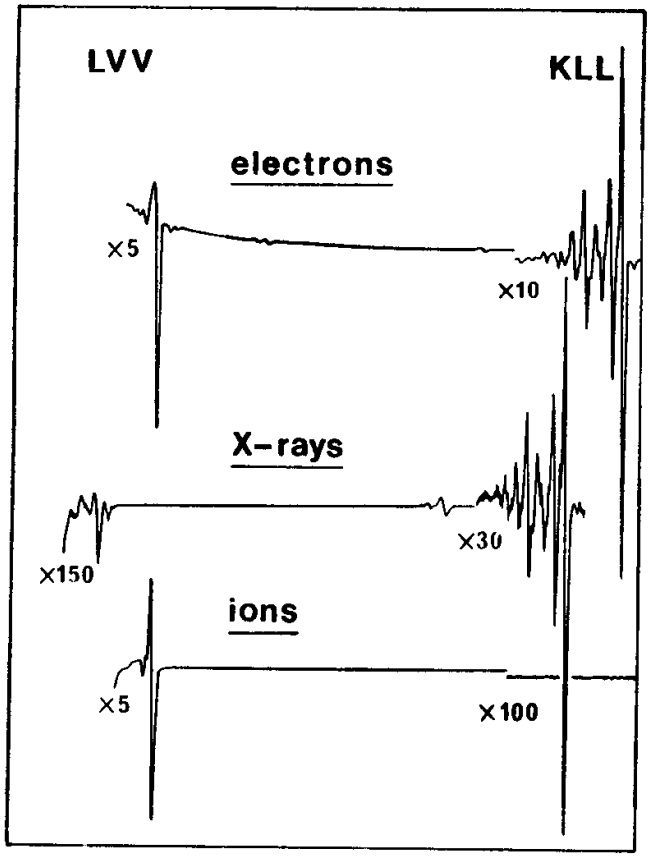

Figure 6.6. Aluminum *LVV* and *KLL* first-derivative Auger spectra under electron (5 keV), x-ray (1254 eV), and ion (5 keV argon) irradiation. The x-ray-induced spectrum is displaced slightly on the energy axis to avoid confusion. The main features to note are: (i) Relatively weak x-ray-induced Auger emission. The *KLL* features are excited, not by the 1254-eV radiation, but by the background bremstrahlung component of the x-ray spectrum. The *LVV* features are very weak due to the low photoionization cross section of the aluminum *L* levels at 1254 eV. (ii) The absence of *KLL* Auger features in the ion-induced spectrum. The ion-induced *LVV* feature, however, is very intense and different in structure to the corresponding electron-induced feature.

Manifestation of change in electronic structure

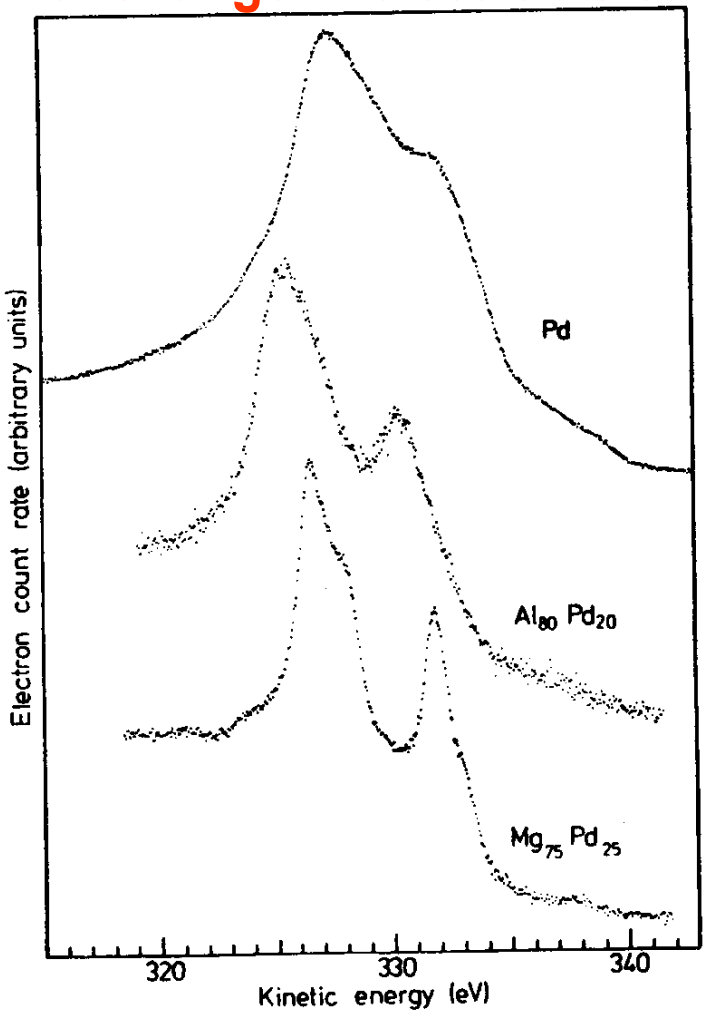

Figure 6.7. Pd $M_{4,5}N_{4,5}N_{4,5}$ Auger spectra from Pd, $Al_{0.8}Pd_{0.2}$, and $Mg_{0.75}Pd_{0.25}$, showing bandlike structure in the element, and atomic-like structure in the alloys. (Reproduced with permission from Reference 140, © Institute of Physics.)

Seggregation

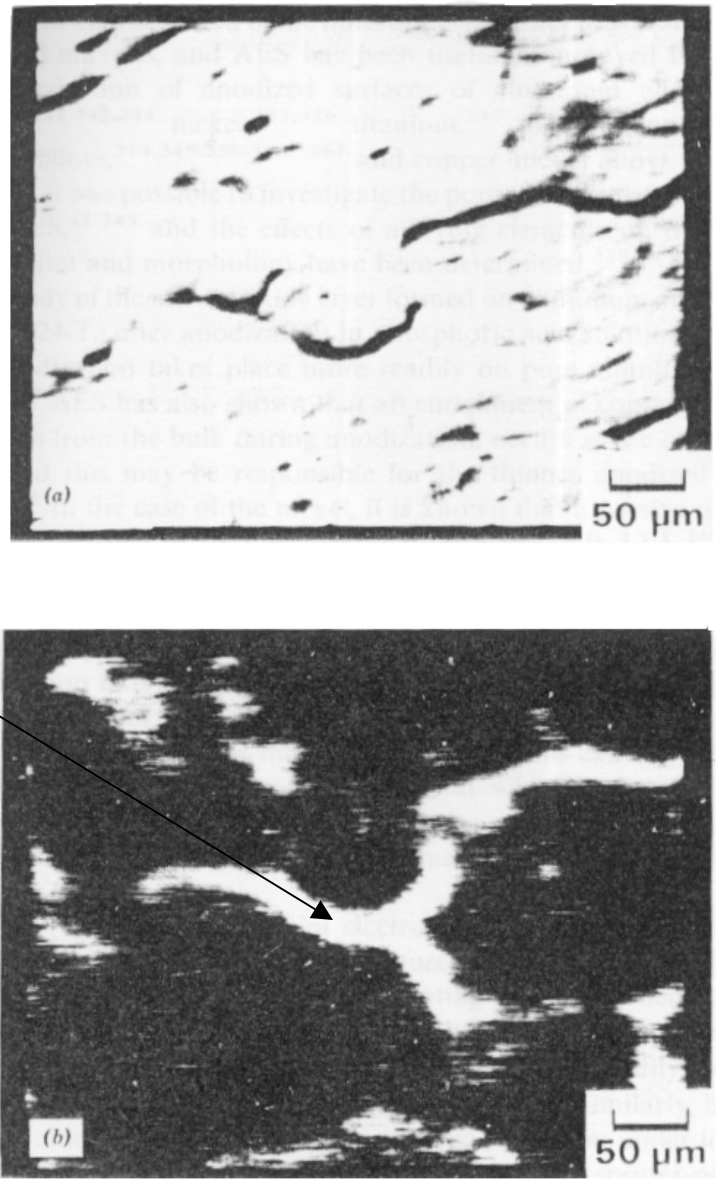

Figure 6.11. (*a*) Secondary-electron image and (*b*) chromium Auger map of 304 stainless steel oxidized in 0.05 torr O_2 at 800 C, showing chromium enrichment at grain boundaries. (Reproduced with permission from Reference 316, © North-Holland Publishing Company.)

Depth profiling

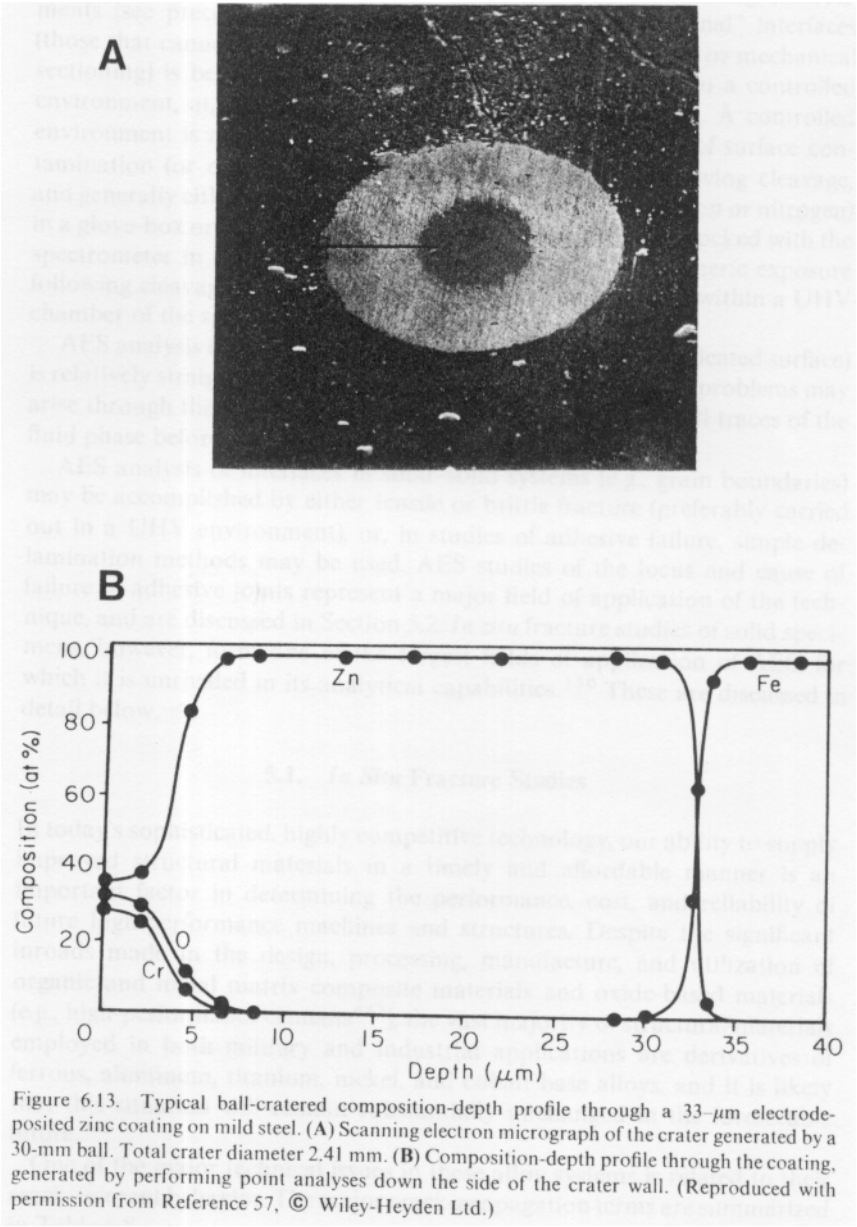

Figure 6.13. Typical ball-cratered composition-depth profile through a 33-μm electrodeposited zinc coating on mild steel. (**A**) Scanning electron micrograph of the crater generated by a 30-mm ball. Total crater diameter 2.41 mm. (**B**) Composition-depth profile through the coating, generated by performing point analyses down the side of the crater wall. (Reproduced with permission from Reference 57, © Wiley-Heyden Ltd.)

Auger spectra can be collected in the normal mode as well.

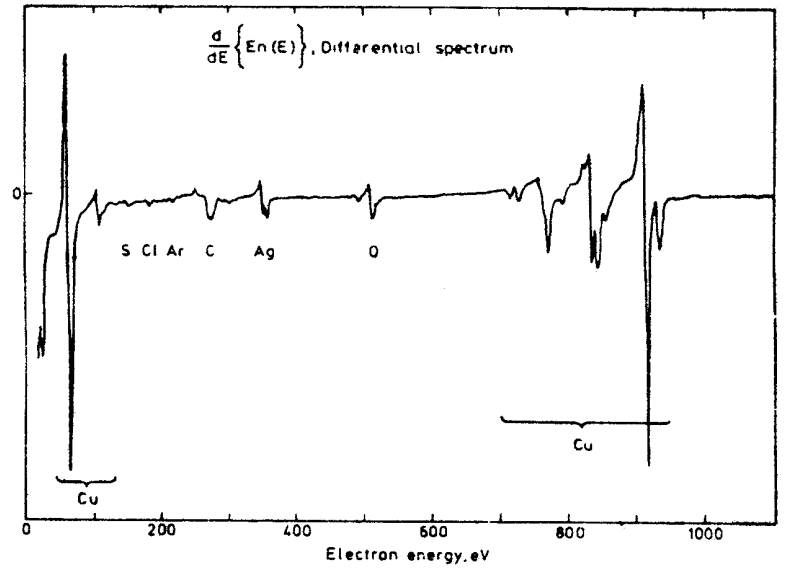

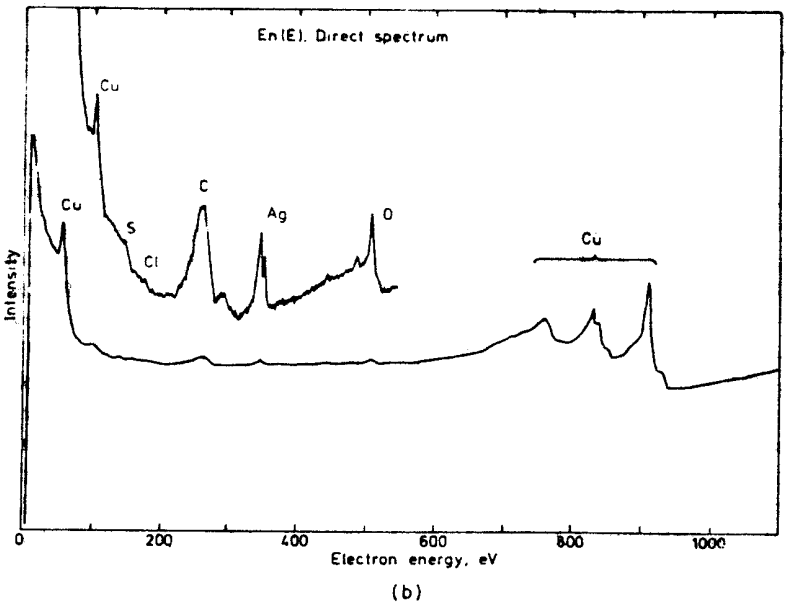

Figure 5.11 Differential and direct electron spectra from contaminated copper

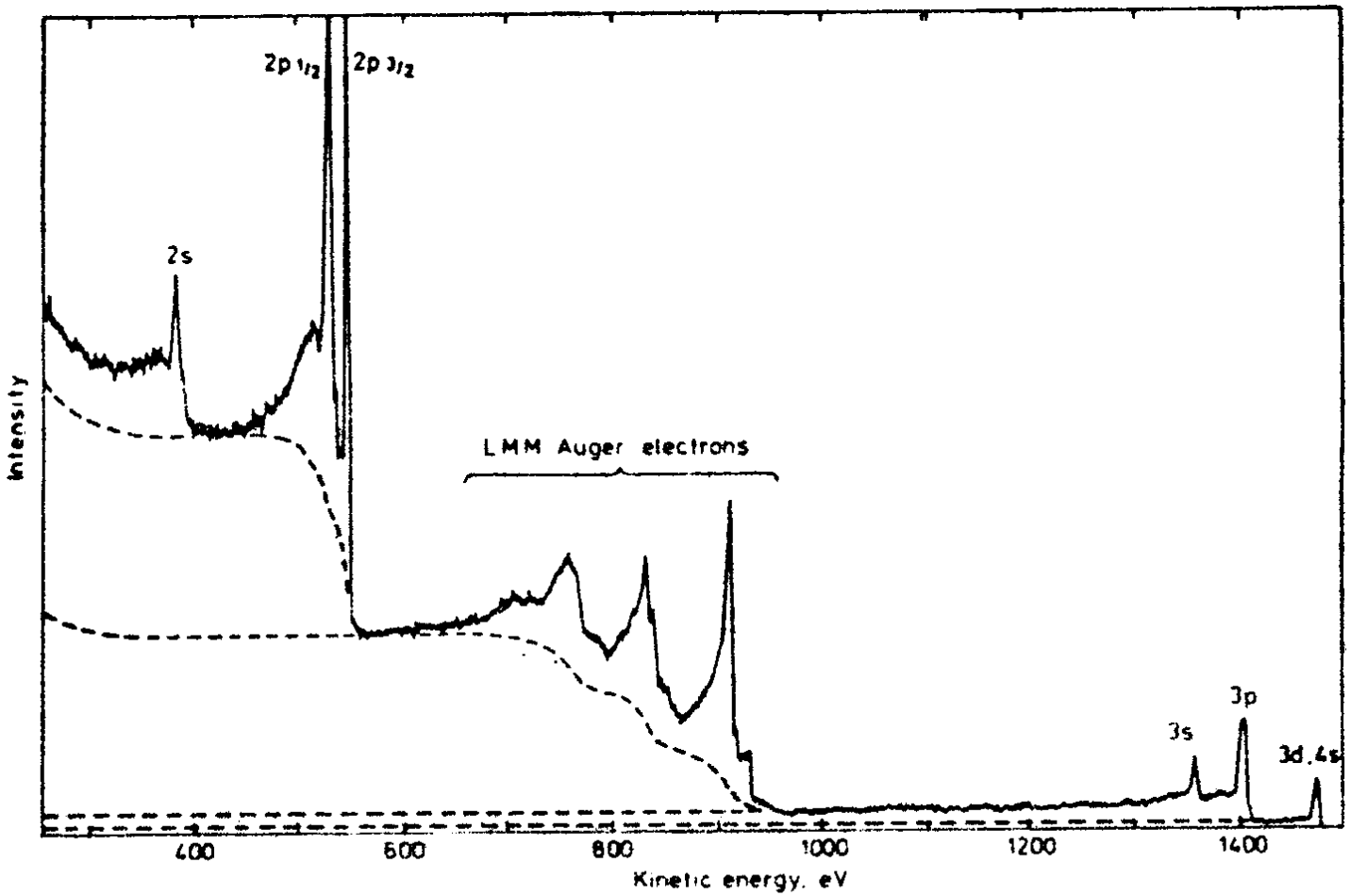

Figure 5.12 XPS spectrum from copper showing the stepped background and Auger electron peaks. (After Seah[21]).

In order to do quantitative analysis, one needs to correct the background.

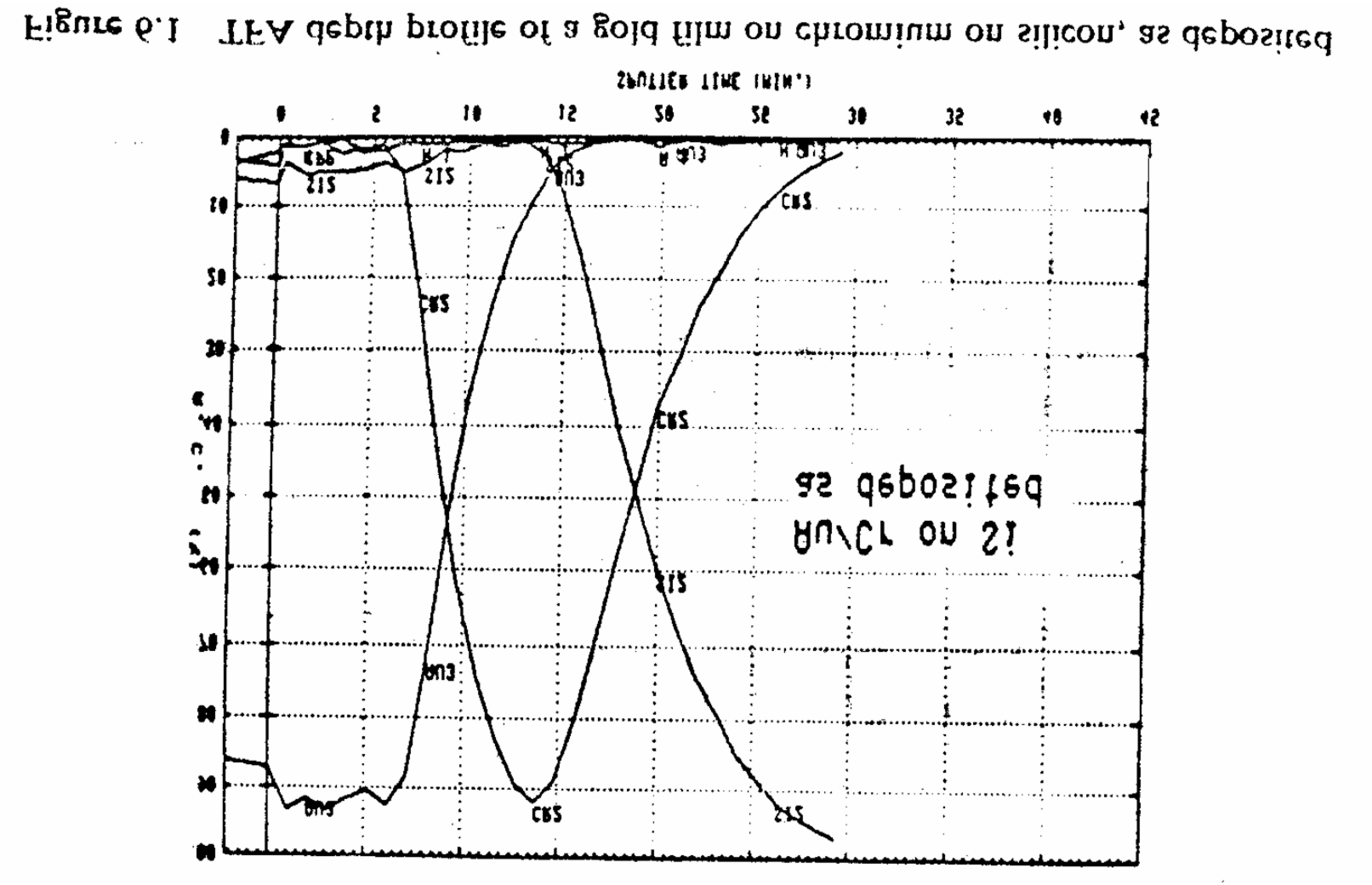

Depth profiling is an important aspect of Auger spectroscopy. The depth resolution can be as high as 50 nm.